

Radio-ejection and bump-related orbital period gap of millisecond binary pulsars

F. D'Antona,¹ P. Ventura¹, L. Burderi², T. Di Salvo³, G. Lavagetto³, A. Possenti⁴ & A. Teodorescu⁵

¹*INAF Osservatorio Astronomico di Roma, via Frascati 33, 00040 MontePorzio, Italy;*
dantona@oa-roma.inaf.it

²*Universit di Cagliari, Cagliari, Italy*

³*Universit di Palermo, Palermo, Italy*

⁴*INAF Osservatorio di Cagliari, Cagliari, Italy*

⁵*Universit di Tor Vergata, Roma*

ABSTRACT

The monotonic increase of the radius of low mass stars during their ascent on the red giant branch halts when they suffer a temporary contraction. This occurs when the hydrogen burning shell reaches the discontinuity in hydrogen content left from the maximum increase in the convective extension, at the time of the first dredge up, and produces a well known “bump” in the luminosity function of the red giants of globular clusters. If the giant is the mass losing component in a binary in which mass transfer occurs on the nuclear evolution time scale, this event produces a temporary stop in the mass transfer, which we will name “bump related” detachment. If the accreting companion is a neutron star, in which the previous mass transfer has spun up the pulsar down to millisecond periods, the subsequent mass transfer phase may be altered by the presence of the energetic pulsar. In fact, the onset of a radio-ejection phase produces loss of mass and angular momentum from the system. We show that this sequence of events may be at the basis of the shortage of systems with periods between ~ 20 and ~ 60 days in the distribution of binaries containing millisecond pulsars. We predict that systems which can be discovered at periods into the gap should have preferentially either magnetic moments smaller than $\sim 2 \times 10^{26} \text{ Gcm}^3$, or larger than $\sim 4 \times 10^{26} \text{ Gcm}^3$. We further show that this period gap should not be present in population II.

Subject headings: pulsars (millisecond) — stars: evolution — stars: interiors

1. Introduction

The basic evolution of low mass X-ray binaries above the ‘bifurcation period’ (Tutukov et al. 1985; Ergma 1996) has been often described (e.g. Webbink et al. 1983). The endpoint of this evolution is a wide system (orbital period P_{orb} from a few to hundreds of days) containing a millisecond pulsar (MSP, the neutron star primary of initial mass M_1 spun up by mass transfer from the secondary, of initial mass M_2) and a low mass helium white dwarf, remnant helium core of the mass losing red giant. The simple relation connecting the giant stellar radius with the helium core mass of the star, which has a very slight dependence on the stellar mass and on the chemical composition, coupled with the Kepler law, produces a relation between the final white dwarf mass M_{WD} and the final P_{orb} , which has been often studied (e.g. Tauris 1996; Rappaport et al. 1995; Tauris & Savonije 1999) and compared with the P_{orb} vs. M_{WD} distribution of the more than 60 known MSPs. The sample of binary MSP known up today shows a shortage of systems with orbital periods between 22 and 56 days. There have been two main attempts to explain this ‘period gap’. According to Tauris (1996), the gap is related to the bifurcation period, which he assumes to be around 2 days. Systems of secondary mass $M_2 \lesssim 1.4M_{\odot}$, and beginning mass transfer just above 2 days period, should evolve to final $P_{\text{orb}} \gtrsim 60$ days. If the secondary has an initial mass $\gtrsim 1.4M_{\odot}$, the binary might evolve through a second common envelope phase, ending at $P \lesssim 20$ days. Taam et al. (2000) revise this picture attributing the periods shorter than 20 days to early massive case B evolution. They question the idea that the bifurcation period is as large as 2 days (to allow a minimum final period larger than 60 days), as evolution towards shorter periods for systems below (but close to) 2 days requires a very strong magnetic braking. Taam et al. (2000) then attribute the period gap to the small range of initial core masses involved ($0.17 \lesssim M_c/M_{\odot} \lesssim 0.2$). In this latter scenario, a carbon oxygen white dwarf of mass larger than $0.35M_{\odot}$ should be present at periods shorter than 20 days. Notice that the two best determined masses are $0.258^{+0.028}_{-0.016}$, at $P_{\text{orb}}=12.3\text{d}$ (Kaspi et al. 1994) and $0.237^{+0.013}_{-0.022}M_{\odot}$, at $P_{\text{orb}}=5.741\text{d}$ (van Straten et al. 2001), so the standard case B evolution produces at least some systems below 20d.

We reconsider the evolution of the systems containing a neutron star and a giant of low initial mass. We only consider the systems in which the initial secondary mass is smaller than the primary mass, in the range $M_{1,in} = 1.2 - 1.35M_{\odot}$, and assume population I composition (metal mass fraction $Z=0.02$)¹.

For a wide range of initial periods, the systems suffer a phase of detachment, when the

¹For larger masses we have an initial phase of mass transfer on the thermal timescale, producing an initial shrinkage of the orbit, until the mass ratio is reversed and the evolution proceeds to longer periods.

hydrogen burning shell reaches the point of deepest penetration of the convective envelope at the basis of the red giant branch (Thomas 1967; Iben 1968). When the hydrogen content suddenly increases, there is a thermal readjustment of the shell physical conditions, with a decrease in the shell temperatures and, consequently, in the nuclear burning luminosity. Thus the star contracts in order to adjust to the level of nuclear reactions in the shell. This phase is an important evolutionary tool in the single star evolution, as the radius contraction is associated to a drop in the luminosity along the red giant branch, producing a “bump” in the luminosity function of simple stellar populations, which has been observed in many globular clusters (Ferraro et al. 1999; Zoccali et al. 1999). It has also been often identified in binary evolution (Kippenhahn et al. 1967; Webbink et al. 1983; Kolb & Ritter 1990), although never discussed in the context of the evolution leading to MSP.

We show that the bump related detachment of the system occurs for a good fraction of the evolutionary paths leading to long period binary MSP, and consider the possible consequences for the orbital period evolution. Although we do not follow explicitly the spin-up evolution of the accreting neutron star, we consider that, when the system resumes mass transfer, the NS is now a millisecond pulsar. Therefore, mass accretion on the NS may be inhibited by the radio-ejection due to the pressure exerted by the MSP radiation on the matter at the inner lagrangian point (Ruderman, Shaham & Tavani 1989; Shaham & Tavani 1990; Burderi et al. 2001; Burderi, D’Antona & Burgay 2002). This alters the binary evolution, as the mass is lost from the system carrying away a specific angular momentum (AM) larger than the average. In fact, the AM lost should be of the order of magnitude of the AM of the donor, whose mass at this stage is only $0.4\text{--}0.5M_{\odot}$, much smaller than the NS mass.

We model parametrically the evolution in the phase of radioejection, and show that it naturally leads, in many cases, the final periods of systems away from the range 20–60 days. We also show that, if the onset of radio-ejection is the mechanism which produces the period gap, this gap should not be found in population II. Unfortunately, the orbital period distribution in globular cluster seems to be altered by destruction mechanisms at long orbital periods, so that this hypothesis by now can not be tested. As a byproduct, we also show that the relation P_{orb} vs. M_{WD} obtained for population I in the framework of the computed models is consistent with the three best observational data.

2. The standard evolution for Population I

We build up our stellar models by the ATON2.1 code, whose input physics is described in Ventura et al. (1998), while the binary evolution routines follow the description in D’Antona

et al. (1989). The code has been recently updated also including explicitly the evolution of the NS (Lavagetto et al. 2004). Models of 1.1 , 1.2 and $1.3M_{\odot}$, with helium mass fraction $Y=0.28$ and metallicity $Z=0.02$, were evolved as donors in binaries containing a NS companion of initial mass in the range 1.2 – $1.35M_{\odot}$. The initial separation was chosen to allow mass transfer at different stages along the evolution. We do not discuss the previous evolution of these putative systems, that is the formation of the neutron star via the supernova (SN) ejection, and whether it is possible to obtain a neutron star in circular orbit with a low mass companion at the periods from which we begin considering the mass transfer. In particular, the common envelope phase preceding the SN event is likely to end with short orbital periods for low mass companions, and long period systems (e.g. $P>100d$) would be created mainly as a consequence of strong natal kicks (see, e.g. Podsiadlowski et al. 2004) and have strong eccentricities.

In addition to nuclear evolution, we assume that magnetic braking is active and describe it according to Verbunt & Zwaan (1981), with the f parameter fixed at 0.5. We also computed several evolutions of systems of $M=0.9M_{\odot}$ and $1.1M_{\odot}$, for $Y=0.24$ and $Z=10^{-3}$ to test the different behavior of population II systems. Table 1 reports some parameters for the binary evolutions starting from different initial models along the evolution of the $1.1M_{\odot}$ as single star, labeled by the model number N_{in} . Smaller N_{in} thus correspond to earlier evolutionary stages. We computed “standard” evolutions, which, at least during the first phase of mass transfer, neglect the possible role of the pulsar. A series of models (labeled by “con” in Table 1) assume conservative mass transfer below the Eddington limit. The matter exceeding the Eddington limit was assumed to be lost from the system, carrying away the specific AM (j_1) of the NS. We considered also evolutions, (labeled by “eta”) in which only a fraction $\eta = 0.5$ of the mass lost by the donor was transferred to the NS, and the remaining half was assumed to leave the system, carrying away the specific AM j_1 . We add several evolutions in which we start again from the bump-related detachment, and assume that all the mass lost from the donor is lost from the system, taking away a large fraction (from 60% to 100%) of the specific AM j_2 of the donor: this is the way in which we simulate an efficient onset of radio-ejection, as this mechanism stops the matter at the inner lagrangian point. Initial and final masses of the components and final periods are also reported in Table 1.

3. The white dwarf and neutron star masses and the final orbital periods

Fig.1 shows the final P_{orb} vs. M_{WD} relation for the population I evolutions of Table 1 (full squares on the left) and for the additional population II models (full squares on the right), and compares them with the analytic approximations provided by Rappaport et al.

(1995) and Tauris & Savonije (1999) for population I and II. Our data compare well with the population II relation by Tauris & Savonije (1999), but it is steeper than theirs at periods $\gtrsim 20$ days for population I. We notice that our population I results are in good agreement with the three observed data points displayed in the figure. These same systems, however, have quite small neutron star masses: the central values for PSR J0437-4715 (van Straten et al. 2001) and B1855+09 (Splaver et al. 2004) are only $1.55\text{--}1.60M_{\odot}$, with upper limits at $\sim 1.7\text{--}1.75M_{\odot}$. In addition, the mass of PSR J1713+0747 (Splaver et al. 2005), at a period of 68d (close to our evolutions 5) is only $1.3\pm 0.2M_{\odot}$. This value is three σ smaller than our predicted mass of $\sim 2.01M_{\odot}$ from sequence 5con, while sequence 5eta provides a much more comfortable value of $1.655M_{\odot}$, as we have assumed the loss of half of the mass lost from the donor, and, in addition, the initial mass of the NS is taken to be only $1.25M_{\odot}$, contrary to the commonplace assumption of a starting value of $1.35\text{--}1.40M_{\odot}$ often adopted in the literature. Notice that the recent accurate mass determination of the relativistic double pulsar system PSR J0737-3039 (Lyne et al. 2004) provides $1.25M_{\odot}$ for the lighter component. To maintain small masses for the pulsar component, we could also have reduced the companion mass down to $1M_{\odot}$. When, on the contrary the initial mass of the donor is somewhat larger than $1.1M_{\odot}$, the first phases will occur at mass transfer rates much larger than Eddington limit, and the additional initial mass will easily be lost from the system. Of course, there is no adequate physical reason to assume the semi-conservative evolution we adopt, but a careful exploration of the parameter space is beyond the purpose of the present work and the results are not affected sensibly by the precise choices. This is shown in Fig 2, which compares the mass loss rate versus period evolution in cases 5con and 5eta. In this standard cases, after the super-Eddington initial phase of mass loss, a stationary phase begins, interrupted by the bump-induced detachment, after which mass loss resumes and follows the same rules. The difference between the conservative and non conservative evolution is not very important, due to the fact that we assume that the specific AM loss associated with the mass loss is that of the primary neutron star, much smaller than the average AM for most of the evolution. The non conservative case, however, allows us to obtain in the end small neutron star masses ($1.6\text{--}1.7M_{\odot}$) much more compatible with the neutron star masses in the systems we are examining. The conservative evolution leads to masses $1.9\text{--}2.1M_{\odot}$. Our following discussion depends on the orbital evolution and not on the assumption of mass conservation, as long as we assume AM is lost from the neutron star.

4. Evolution following the bump detachment: the role of radio-ejection

Fig. 3 shows the HR diagram of the donor star $1.1M_{\odot}$ for $Z=0.02$. The evolutionary track without mass loss is shown as a reference. The location of the bump is seen in the

thickening of the track, at $\log L/L_{\odot} \sim 1.5$. It corresponds to a stage at which the core mass is $\sim 0.218M_{\odot}$. We see that a bump signature is present in all the evolutions where mass loss begins at evolutionary phases at which the hydrogen burning shell has not yet reached the discontinuity in hydrogen left by convection.

At the bump-related detachment, in all cases, the NS has been accelerated by the first phase of mass transfer. We assume that the maximum spin achieved is the observed minimum spin period $P = 1.3\text{ms}$. During the semi detached evolution, the total mass decreases, while the hydrogen shell advances and the H-exhausted core increases in mass, until it will encounter the discontinuity. Of course the earlier is the phase at which mass loss starts, the smaller is the total mass at the time of detachment. When the mass loss rate is resumed, it is much larger if we assume that, thanks to an efficient radio-ejection, the matter lost from the system carries away a large fraction of the specific AM of the donor. Figure 4 shows the different evolutions obtained in cases 4re. The larger is the fraction of specific AM lost, the larger is the mass loss rate, and the shorter is the final P_{orb} . We see that the standard evolution would lead to a final period of ~ 36 days, in the middle of the period gap. But if radio ejection is efficient the period is reduced below 22 days for a fraction between 60% and 80% of AM loss, corresponding to a mass transfer rate of $\sim 5 \times 10^{-9}M_{\odot}/\text{yr}$. We must then understand when and where the mass transfer rates obtained are compatible with the assumption of radio-ejection.

Figure 5 displays the mass transfer rates for cases 3, 4 and 5, and compares the standard evolution with the evolutions assuming that 80% of the donor AM is lost starting after the bump-related detachment. Contrary to the case discussed above, the evolution of case 5 leads to a final period in the middle of the gap ($\sim 28\text{d}$) if there is an efficient radio-ejection, corresponding to a mass loss rate of $2 \times 10^{-8}M_{\odot}/\text{yr}$, otherwise the final period is $\sim 61\text{d}$, at the upper end of the period gap.

5. Constraints for the magnetic momentum of the pulsar

Which are the constraints on the pulsar magnetic field which allow an efficient radio-ejection in case 4 and non efficient in case 5? We assume that the maximum spin frequency attainable by the MSP is $\sim 750\text{Hz}$ (Chakrabarty et al. 2003) (corresponding to a minimum period of $\sim 1.3\text{ms}$). Following Burderi et al. (2001), we remember that radio-ejection can occur for orbital periods longer than the critical period:

$$P_{\text{orb,crit}} = 0.7 \times (\alpha^{-36} n_{0.615}^{-40})^{3/50} \dot{m}_{-10}^{51/25} m^{107/50} \times \\ \mu_{26}^{-24/5} P_{\text{spin},-3}^{48/5} \left[1 - 0.462 \left(\frac{m_2}{m + m_2} \right)^{1/3} \right]^{-3/2} \times \\ (m + m_2)^{-1/2} \text{ h} \quad (1)$$

where α is the Shakura–Sunyaev viscosity parameter, μ_{26} is the magnetic moment of the neutron star in units of 10^{26} Gauss cm³ (corresponding to a surface magnetic field of 10^8 Gauss), $P_{\text{spin},-3}$ is the spin period of the neutron star in milliseconds, $n_{0.615} = n/0.615 \sim 1$ for a gas with solar abundances (where n is the mean particle mass in units of the proton mass m_p), \dot{m}_{-10} is the accretion rate in units of $10^{-10} M_\odot/\text{yr}$. This critical period has been derived equating the pressure of a Shakura-Sunyaev accretion disc (approximately proportional to $r^{-2.6}$) with the radiation pressure exerted by the magneto-dipole rotator (proportional to r^{-2}). This gives a radius beyond which radiation pressure always dominates over disk pressure, causing the ejection of matter of the disc. Equating this radius with the distance between the NS and the inner lagrangian point, which we approximate with the difference between the orbital separation and the Roche lobe radius of the secondary (which depends on the binary period), and solving for the orbital period gives a critical period beyond which accretion is always inhibited by the action of the pulsar pressure. We can invert Equation 1 to obtain the value of the critical magnetic momentum as a function of the critical orbital period: we obtain

$$\mu_{26} = 0.93 A^{1/80} \dot{m}_{-10}^{51/120} m^{107/240} P_{\text{spin},-3}^2 P_{\text{orb,crit}}^{-5/24} B^{-5/16} (m + m_2)^{-5/48} \text{Gcm}^3 \quad (2)$$

where $A = \alpha^{-36} n_{0.615}^{-40}$, a value close to 1, and $B = 1 - 0.462(m_2/(m + m_2))$. Assuming that the NSs have been accelerated to the minimum observed spin period $P_{\text{spin},-3} = 1.3\text{ms}$, inserting the appropriate values for the masses (see table 1), and assuming that the orbital period at the bump is the critical period, we can derive a constraint on the magnetic moment of the NS. Namely, if we wish that the sequence 4 experiences radio–ejection (to reduce its final period below 22d) while sequence 5 does not (to avoid a final period into the gap), we must impose:

$$2 \times 10^{26} \lesssim \mu \lesssim 4 \times 10^{26} \text{Gcm}^3 \quad (3)$$

for those systems whose initial binary parameters would lead them into the period gap. In this interpretation, the gap is only a statistical gap, and not a forbidden region. Therefore, we can predict that systems with P_{orb} into the gap can exist, but they should preferentially have magnetic moments out of the interval given in Eq.2. Fig. 6 reports the orbital periods

vs. the magnetic moments for all the known binary MSPs in the galactic field (as derived from version 1.32 of the ATNF pulsar catalog², and from Stairs et al. 2005) having spin period shorter than 10 ms, $P_{\text{orb}} > 3$ d, nearly circular orbit (eccentricity smaller than 10^{-3}) and supposedly white dwarf companion of mass $\lesssim 0.4 M_{\odot}$. The aforementioned parameters are the typical outcomes of the standard nuclear evolution of low mass X-ray binary, which is in the focus of this paper (e.g. Webbink et al. 1983). It appears that about 75% of the sample displays magnetic moments within the range of equation 2 or very close to its limits. The evolution of the three systems at $P_{\text{orb}} \sim 13$ days might have been influenced by radio ejection, and the two systems at $P_{\text{orb}} \sim 56$ days could have been found in the gap, if their magnetic moments had been larger.

The proposed scenario is finally summarized in Fig. 7, reporting the evolution in the plane P_{orb} vs. white dwarf mass. We see that, taking into account the NS evolution and the process of radio–ejection leads to a natural explanation of the period gap. A population synthesis may give further support to this picture, allowing to precisely calculate the effect of the interplay between the various parameters in eq. 1 on the P_{orb} vs μ distribution.

6. Population II models

The result we have found derives from three main occurrences: 1) the maximum extension of the convective envelope in population I reaches down to an inner mass point of $\sim 0.24 M_{\odot}$, so that the bump induced detachment occurs when the hydrogen exhausted core mass reaches about $0.22 M_{\odot}$, at a period well below 20 days for the systems in which we have tested that the radio–ejection mechanism can work. In population II, the maximum extent of convection only reaches $\sim 0.35 M_{\odot}$. Thus any bump related detachment would occur at a much longer orbital period, when the core reaches $\gtrsim 0.3 M_{\odot}$ and the red giant has already transferred a large amount of its envelope. Therefore, even if radio–ejection begins to dominate, it can not affect in an interesting way the binary final period. In any case, no period gap can occur due to this mechanism, for periods shorter than ~ 35 days.

Unfortunately, the globular cluster period distribution (Camilo & Rasio 2005) does indicate that it is affected by the dynamic encounters in the dense stellar environment. In particular, systems with period larger than 10 days are so few that we can not falsify our hypothesis by now.

²<http://www.atnf.csiro.au/research/pulsar/psrcat>

7. Conclusions

We follow the evolution of the mass losing component in systems progenitors of binaries containing a MSP and a remnant white dwarf companion. When the mass transfer begins during the red giant branch phase, in many cases the binary evolution shows a period of detachment, due to the shrinking of the stellar radius which occurs when the hydrogen burning shell meets with the hydrogen discontinuity left at the time of the maximum extension of the convective envelope. When the mass transfer resumes, it is possible that the evolution suffers a radio-ejection phase which alters the final orbital parameters, due to the loss of mass and AM from the system. We show that the period gap between 22 and 56 days in the distribution of binary MSPs is produced if the magnetic momentum of the neutron star is in the range $\sim 2 - 4 \times 10^{26} \text{ Gcm}^3$, typical of MSPs. A population synthesis study could strengthen the conclusion that this period gap is "bump-related", but there are many parameters to be considered in the analysis. A better test of the model would be if new systems are found into the period gap, and their magnetic moments are either below $\sim 2 \times 10^{26} \text{ Gcm}^3$, or above $\sim 4 \times 10^{26} \text{ Gcm}^3$.

This research was supported by PRIN 2003 "Pushing ahead the frontiers of pulsar research".

REFERENCES

Burderi, L. et al. 2001, ApJ, 560, L71
Burderi, L., D'Antona, F. & Burgay, M. 2002, ApJ, 574, 325
Camilo, F. & Rasio, F.A. 2005, in "Binary Radio Pulsars" ASP Conference Series, Vol. 328, 2005 F. A. Rasio and I. H. Stairs, eds., in press
Chakrabarty, D. et al. 2003, Nature 424, 42
D'Antona, F., Mazzitelli, I., & Ritter, H. 1989, A&A, 225, 391
Ergma, E. 1996, A&A, 315, L17
Ferraro F.R., Messineo M., Fusi Pecci F., De Palo M.A., Straniero O., Chieffi A., & Limongi M. 1999, AJ, 118, 1738
Iben I. Jr. 1968, Nature, 220, 143

Kaspi, V. M., Taylor, J. H., & Ryba, M. 1994, ApJ, 428, 713

Kippenhahn, R., Kohl, K., & Weigert, A. 1967, Zeitschrift fur Astrophysics, 66, 58

Kolb, U., & Ritter, H. 1990, A&A, 236, 385

Lavagetto, G., Burderi, L., D'Antona, F., Di Salvo, T., Iaria, R., & Robba, N. R. 2004, MNRAS, 348, 73

Lyne, A. G., et al. 2004, Science, 303, 1153

Podsiadlowski, P., Langer, N., Poelarends, A. J. T., Rappaport, S., Heger, A., & Pfahl, E. 2004, ApJ, 612, 1044

Rappaport, S., Podsiadlowski, P., Joss, P. C., Di Stefano, R., & Han, Z. 1995, MNRAS, 273, 731

Ruderman, M., Shaham, J. & Tavani, M. 1989, ApJ, 336, 507

Shaham, J. & Tavani, M. 1990, ApJ, 377, 588

Splaver, E. M. 2004, Ph.D. Thesis, Princeton University, Princeton, N.J. USA

Splaver, E. M., Nice, D. J., Stairs, I. H., Lommen, A. N., & Backer, D. C. 2005, ApJ, 620, 405

Stairs, I. H., Faulkner, A. J., Lyne, A. G., Kramer, M., Lorimer, D. R., McLaughlin, M. A., Manchester, R. N., Hobbs, G. B., Camilo, F., Possenti, A., Burgay, M., D'Amico, N., Freire, P. C., Gregory, P. C. 2005, ApJ, in press, astro-ph/0506188

Taam, R. E., King, A. R., & Ritter, H. 2000, ApJ, 541, 329

Tauris, T. M. 1996, A&A, 315, 453

Tauris, T. M., & Savonije, G. J. 1999, A&A, 350, 928

Thomas, H.-C. 1967, Zeitschrift fur Astrophysics, 67, 420

Tutukov, A. V., Fedorova, A. V., Ergma E., & Yungelson, L. R. 1985, *Soviet Astron. Lett.*, **11**, 123

van Straten, W., Bailes, M., Britton, M., Kulkarni, S. R., Anderson, S. B., Manchester, R. N., & Sarkissian, J. 2001, Nature, 412, 158

Ventura, P., Zeppieri, A., Mazzitelli, I., & D'Antona, F. 1998, A&A, 334, 953

Verbunt, F., & Zwaan, C. 1981, A&A, 100, L7
Webbink, R. F., Rappaport, S., & Savonije, G. J. 1983, ApJ, 270, 678
Zoccali M., Cassisi S., Piotto G., Bono G., & Salaris M. 1999, ApJ, 518, L49

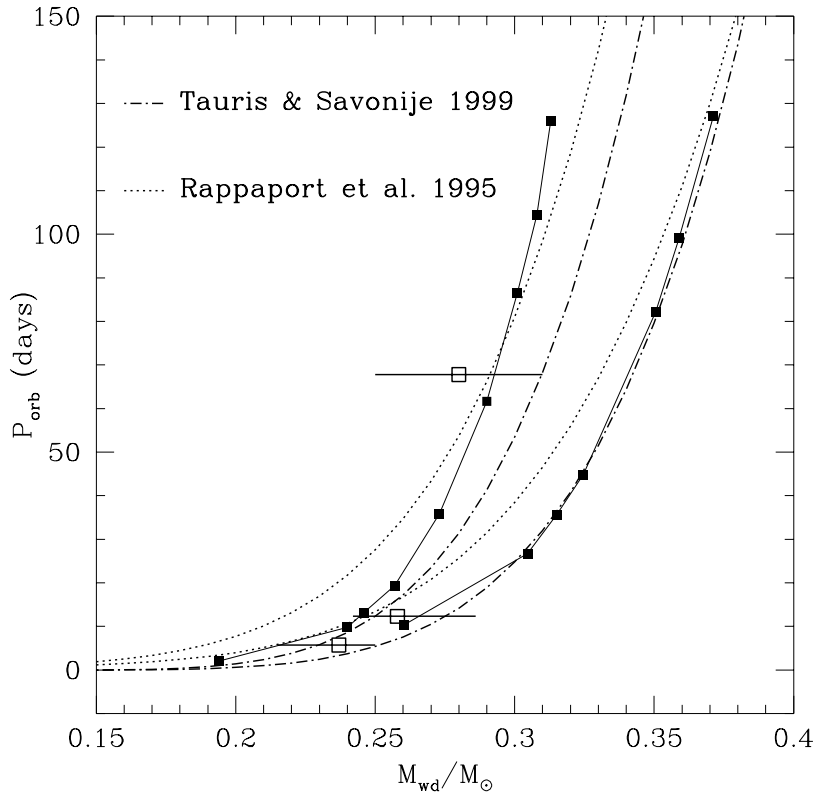


Fig. 1.— In the plane P_{orb} vs. M_{WD} , the result of our computations (full squares) are compared to the analytic relations by Rappaport et al. (1995) and Tauris & Savonije (1999). The three curves on the left represent the results for population I, and the three curves on the right are for population II. The three open squares with error bars show three MSP binaries for which masses of the white dwarf component are well determined: PSR J1713+0747 (Splaver et al. 2005) at $P=67.825$ d, B1855+09 (Kaspi et al. 1994) at $P=12.327$ d, and J0437-4715 (van Straten et al. 2001) at $P=5.741$ d. These three systems are well compatible with the white dwarf mass vs. period relation of our models.

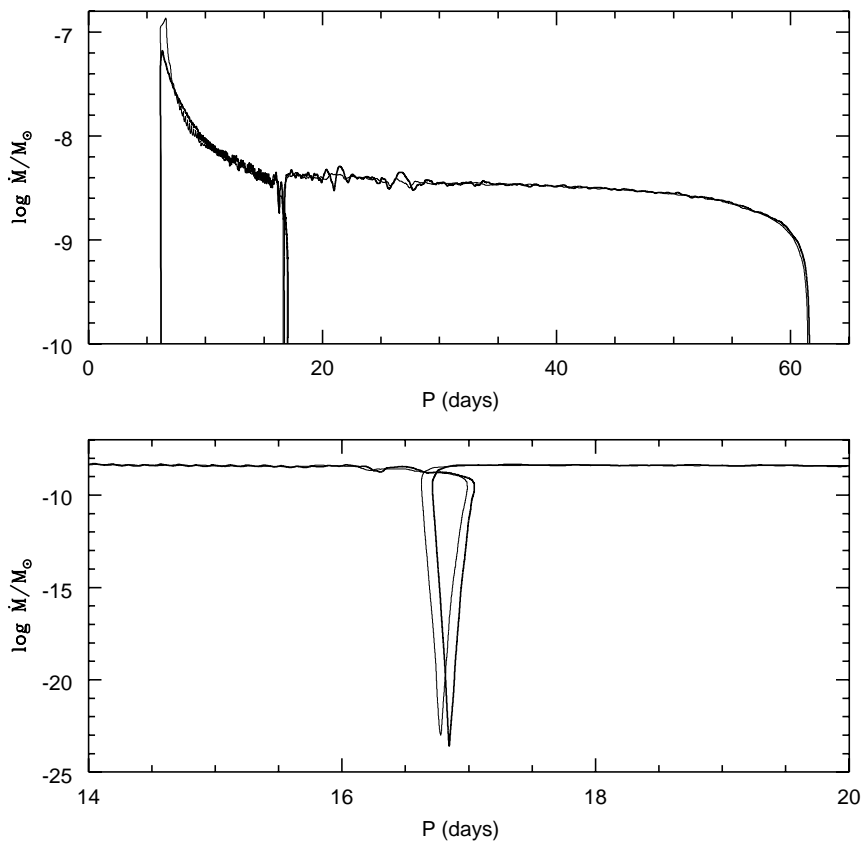


Fig. 2.— Comparison of mass transfer rate vs. period for evolutions 5con and 5eta, differing for the modalities of mass transfer. The bottom panel shows an enlargement at the detachment period. During detachment the orbital period decreases due to the magnetic braking.

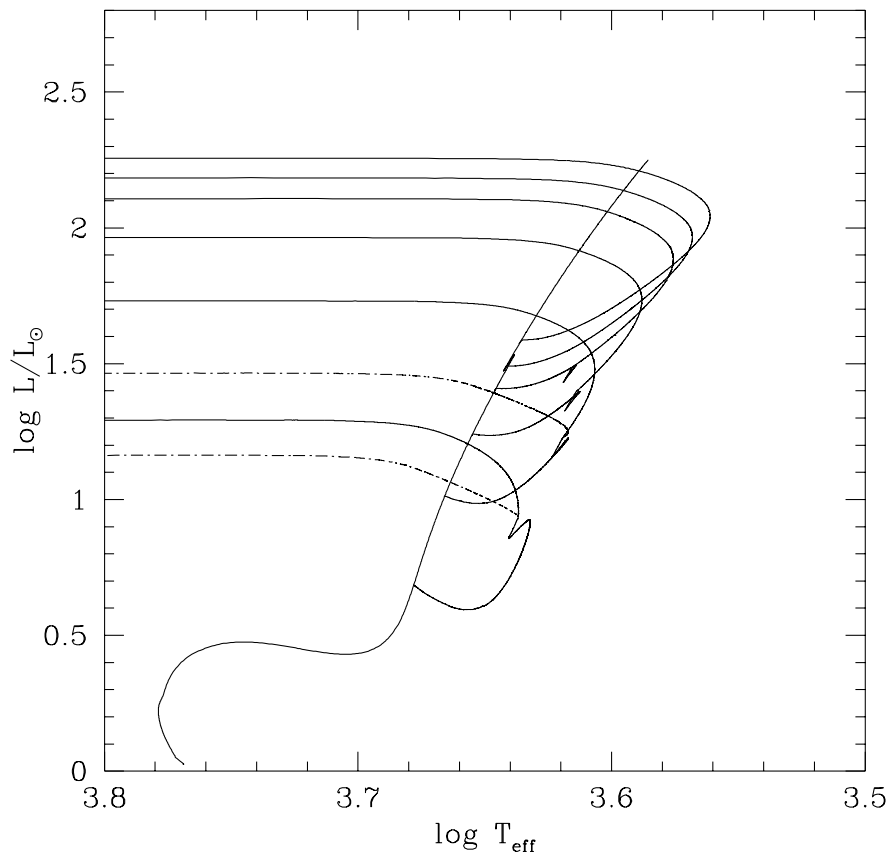


Fig. 3.— HR diagram of the single $1.1M_\odot$ evolution and of the binary evolutions from 3con to 9con in Table 1, starting in order at increasing luminosities along the track. The tracks starting below the bump show a bump signature. The dashed curves starting at the bump of sequences 3con and 4con are sequences 3re and 4re08.

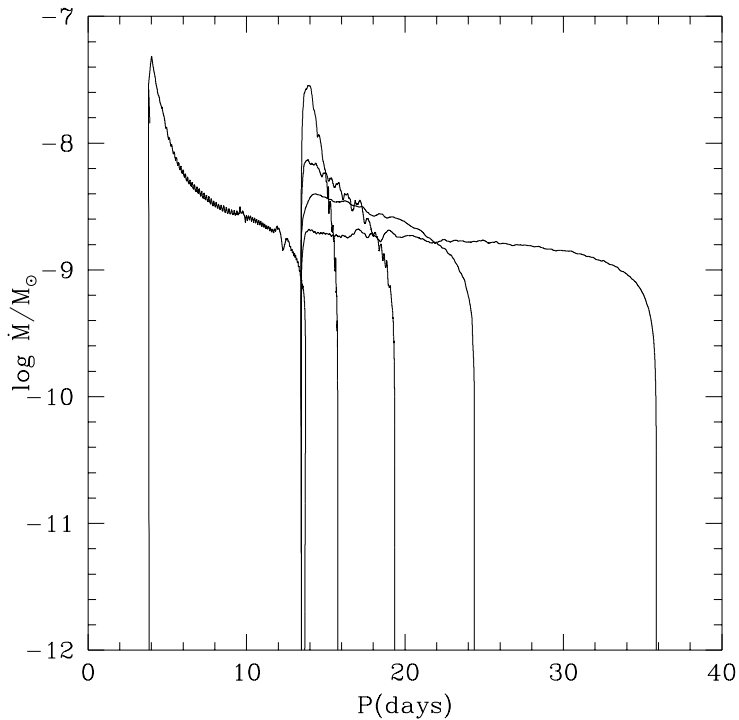


Fig. 4.— Mass loss rate vs. orbital period for the “standard” sequence 4, track starting at the shortest period and ending, after the detachment, at the longest period. After the bump-induced detachment, three other tracks are shown, in which all the mass is lost from the system, carrying away 60%, 80% or 100% of the specific AM of the donor. The larger is the AM loss, the larger is the mass transfer rate, and the shorter is the final orbital period. If the AM loss is between 60 and 80%, the final period is in the range 20–24d.

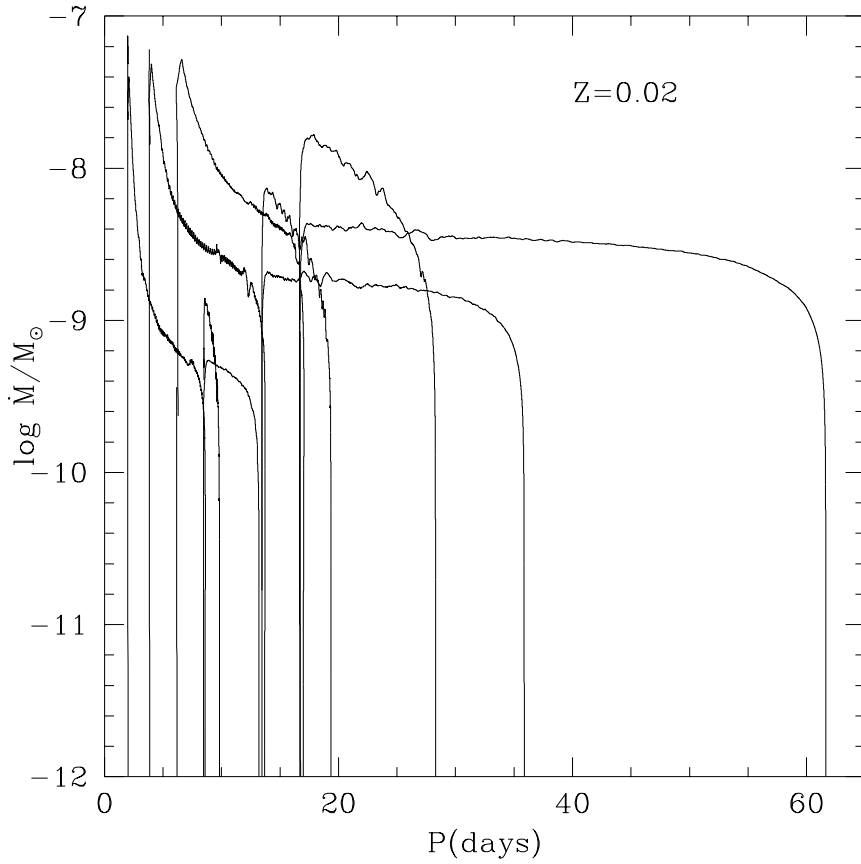


Fig. 5.— Mass loss rate vs. orbital period for the cases 3con, 4con and 5con (from left to right). Starting at the bump detachment, in addition to the standard evolution, we show also the three sequences 3re, 4re08 and 5re08, in which, due to radio-ejection, 80% of the specific AM of the donor star is lost with the mass lost by the system, and a shorter final orbital period is achieved.

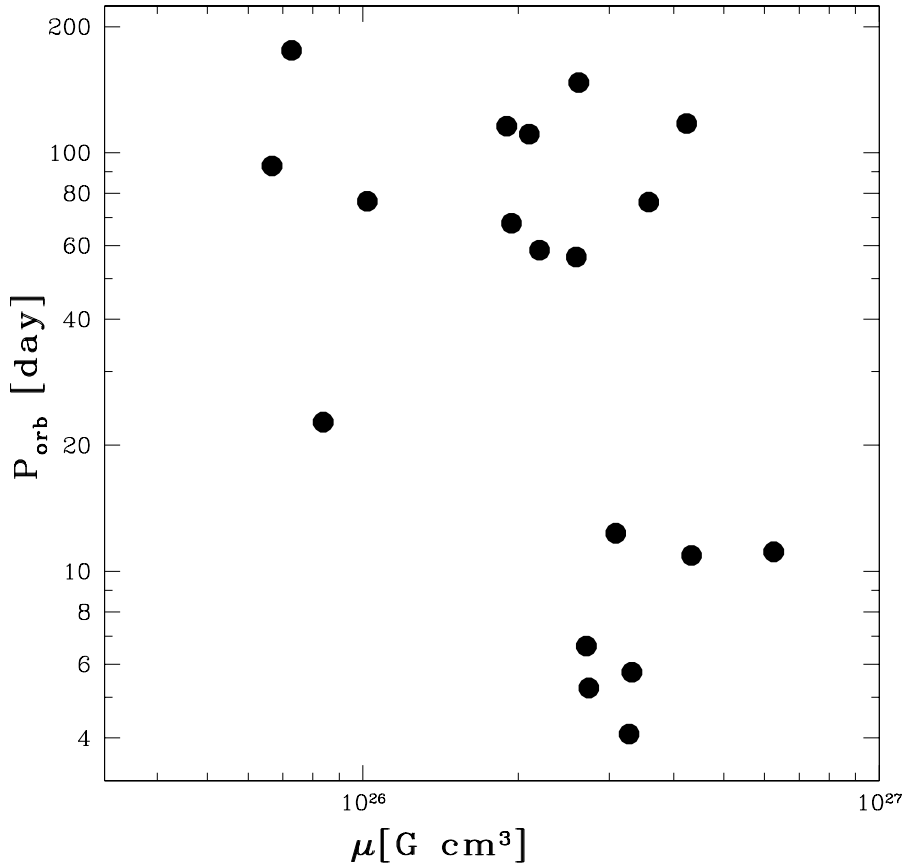


Fig. 6.— Logarithmic plot of orbital periods P_{orb} vs. magnetic moments μ for 19 galactic field MSPs in wide binary systems, whose companion is expected to be a moderately massive white dwarf. The other selection criteria are listed in the text. The shortage of systems with orbital period in the interval between ~ 20 d and ~ 60 d is evident. All the values of μ are calculated assuming a moment of inertia 10^{45} g cm 2 for the neutron star and using the formula $\mu = 3.2 \times 10^{37} \sqrt{P \dot{P}}$ G cm 3 , where P and \dot{P} are the pulsar spin period and its time derivative. Corrections to the value of \dot{P} due to the pulsar proper motion have been applied whenever they were available (12 cases over 19).

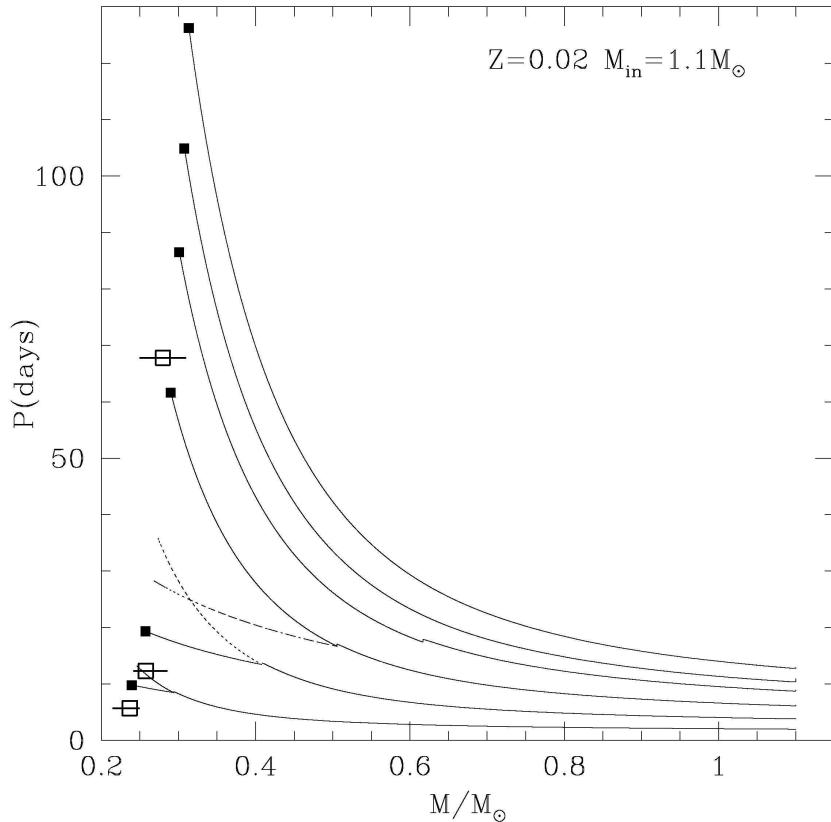


Fig. 7.— Orbital period versus donor mass evolution. For the first three tracks starting from bottom, both the conservative case (3con, 4con and 5con, in order of increasing period) and the cases including radio-ejection, 3re, 4re08, 5re08, beginning at the bump related detachment and ending at a shorter period than the standard tracks) are shown. At larger periods, the cases 6con , 8con and 9con are shown. In order to produce a period gap, as a consequence of the bump-related detachment, in the range 20 – 60 days, the radio-ejection phase should occur for the first and second system from bottom, while it must not occur for the third system (see text). Dots at the end of the sequences indicate which are the white dwarf masses and orbital periods we expect to be result of the evolutions. The three open squares are the systems described in Fig. 1.

Table 1. Models

Seq.	η^a	j ^a	N_{in}	$M_{c,in}^b$	$M_{2,i}$	$M_{1,i}$	M_b^c	$M_{2,f}$	$M_{1,f}$	$P_b(d)^c$	$P_f(d)$	$\log(\dot{M})^d$
2con	1	j ₁	200	0.0511	1.1	1.35		0.194	2.256		2.101	-10.00
3con	1	j ₁	300	0.1550	1.1	1.35	0.293	0.246	2.072	8.52	13.20	-9.27
4con	1	j ₁	400	0.1868	1.1	1.35	0.408	0.273	2.047	13.60	35.86	-8.67
5con	1	j ₁	500	0.2049	1.1	1.35	0.505	0.290	2.012	16.80	61.63	-8.38
6con	1	j ₁	600	0.2184	1.1	1.35	0.617	0.301	1.977	17.67	86.57	-8.11
8con	1	j ₁	800	0.2383	1.1	1.35		0.303	1.959		105.0	-8.05
9con	1	j ₁	900	0.2463	1.1	1.35		0.310	1.939		126.3	-7.85
3eta	.5	j ₁	300	0.1552	1.1	1.20		0.244	1.628	8.14	12.10	-9.27
4eta	.5	j ₁	400	0.1868	1.1	1.35	0.415		1.692	13.64		-8.80
5eta	.5	j ₁	500	0.2049	1.1	1.25		0.290	1.655	16.84	61.49	-8.38
3re	0	0.8j ₂	300	0.2106	0.293	2.025		0.240	2.025		9.817	-8.84
4re06	0	0.6j ₂	400	0.2266	0.408	1.692		0.263	1.692		24.38	-8.42
4re08	0	0.8j ₂	400	0.2266	0.408	1.912		0.257	1.912		19.35	-8.08
4re1	0	j ₂	400	0.2266	0.408	1.692		0.253	1.692		15.75	-7.56
5re08	0	0.8j ₂	500	0.2324	0.505	1.796		0.268	1.796		28.28	-7.77
5re1	0	j ₂	500	0.2367	0.505	1.547		0.261	1.547		21.46	-7.00

^a $\eta = 1$: conservative mass transfer up to $\dot{M}_{Eddington}$, the mass exceeding the Eddington limit is lost from the system. $\eta = .5$: half of the mass lost by the donor is accreted. In both cases, the mass lost from the system takes away the specific AM of the NS j₁. All the cases $\eta = 0$ correspond to the radio-ejection: all the mass lost from the donor is lost from the system, carrying away a percentage of the donor specific AM, j₂, specified in column 3.

^bHelium core mass, in units of M_⊙, when mass transfer begins.

^cMass of the donor and period at the bump-related detachment.

^dUnits: M_⊙/yr. For the sequences from 2 to 9, mass transfer rate in the stationary phase following the peak at the beginning of mass transfer; for the radio-ejection sequences, labelled "re", the peak mass transfer rate at the beginning of the evolution is given.